Vol 18 No 9, September 2009
1674-1056/2009/18(09)/3990-05

Chinese Physics B

© 2009 Chin. Phys. Soc.
and IOP Publishing Ltd

Study on characteristics of a double-conductible channel organic thin-film transistor with an ultra-thin hole-blocking layer*

Yuan Guang-Cai(袁广才)[a)b)], Xu Zheng(徐 征)[a)b)†], Zhao Su-Ling(赵谡玲)[a)b)],
Zhang Fu-Jun(张福俊)[a)b)], Xu Na(许 娜)[c)],
Tian Xue-Yan(田雪雁)[a)b)], and Xu Xu-Rong(徐叙瑢)[a)b)]

[a)] *Institute of Optoelectronics Technology, Beijing Jiaotong University, Beijing* 100044, *China*
[b)] *Key Laboratory of Luminescence and Optical Information (Beijing Jiaotong University), Ministry of Education, Beijing* 100044, *China*
[c)] *School of Sciences, Beijing Jiaotong University, Beijing* 100044, *China*

(Received 30 December 2008; revised manuscript received 21 January 2009)

The properties of top-contact organic thin-film transistors (TC-OTFTs) using ultra-thin 2, 9-dimethyl-4, 7-diphenyl-1, 10-phenanthroline (BCP) as a hole-blocking interlayer have been improved significantly and a BCP interlayer was inserted into the middle of the pentacene active layer. This paper obtains a fire-new transport mode of an OTFT device with double-conductible channels. The accumulation and transfer of the hole carriers are limited by the BCP interlayer in the vertical region of the channel. A huge amount of carriers is located not only at the interface between pentacene and the gate insulator, but also at the two interfaces of pentacene/BCP interlayer and pentacene/gate insulator, respectively. The results suggest that the BCP interlayer may be useful to adjust the hole accumulation and transfer, and can increase the hole mobility and output current of OTFTs. The TC-OTFTs with a BCP interlayer at $V_{DS} = -20$ V showed excellent hole mobility $\mu_{\rm FE}$ and threshold voltage $V_{\rm TH}$ of 0.58 cm^2/(V·s) and –4.6 V, respectively.

Keywords: organic thin-film transistor, ultra-thin hole-blocking layer, double-conductible channels
PACC: 7340, 7340L, 6110M, 7360Q

1. Introduction

Organic thin film transistors (OTFTs) are a promising alternative to amorphous silicon devices. OTFTs are currently developed for low-cost, large area, and flexible electronic applications. The performance of OTFTs has been improved significantly by modifying the dielectric surface and/or source and drain (S/D) electrodes, or by using novel dielectric materials, and the achievement of high-performance OTFTs has mostly been in top-contact (TC) configuration rather than in bottom-contact (BC) configuration in the past decade.[1−4] The OTFT device is a powerful experimental tool to investigate the charge carrier transport properties of organic materials, including the distribution of density of states, charge carrier mobility and stability.[5−9] Pentacene is an interesting organic semiconductor material for use in OTFTs. OTFTs using pentacene films showed a carrier mobility as high as that of hydrogenated amorphous silicon transistors (a-Si:H TFT).[10−12] Other studies have already reported most of above-mentioned questions and obtained good results. However, investigations on multi-conductible channels OTFTs are rare up to the present. In this paper, we mostly investigate the properties of pentacene based on double-conductible channel TC-OTFTs and report a significant improvement on the properties of an OTFT device using ultra-thin hole-blocking as an interlayer (HBI).

*Project supported by the National High Technology Research and Development Program of China (Grant No 2006AA03Z0412), the National Natural Science Foundation of China (Grant Nos 10774013 and 10804006), the Excellent Doctor's Science and Technology Innovation Foundation of Beijing Jiaotong University (Grant No 48024), the Research Fund for the Youth Scholars of the Doctoral Program of Higher Education (Grant No 20070004031), the Beijing NOVA program (Grant No 2007A024), the Project Sponsored by the Scientific Research Foundation for the Returned Overseas Chinese Scholars, State Education Ministry and the Foundation of Beijing Jiaotong University (Grant No 2005SM057).
†Corresponding author. E-mail: zhengxu@bjtu.edu.cn or ygc219@126.com

2. Experiment

All OTFT structures were fabricated on a heavily doped p-type Si wafer with a 300 nm thick complex SiO_xN_y insulator layer fabricated by radio frequency magnetron sputtering. The doped p-type Si wafer functioned as the gate electrode and the complex SiO_xN_y functioned as the gate insulator.

To determine the dielectric properties of the SiO_xN_y gate insulator layer, we prepared a capacitor structure. Gate insulators were sandwiched between the top and bottom electrodes in the capacitor structure by using a gold dot (from vapour) on the gate insulator as the top electrode and gold deposited on the SiO_2/Si substrate as the bottom electrode. The capacitance of the gate insulator was measured with a capacitance–voltage meter and the dielectric constant of the gate insulator was calculated from the capacitance. The dielectric constant and capacitance per unit area of the SiO_xN_y gate insulator were 6.34 and 16.48 nF/cm^2 at room temperature.

3. Results and discussion

We fabricated TC-OTFTs with bottom gate structure on a p-type Si wafer. Firstly, pentacene thin films as active layers were deposited on p-type Si wafer substrate with complex SiO_xN_y insulator by thermal evaporation under high vacuum 2×10^{-5} Pa. Then Au source–drain (S–D) electrodes were deposited on top of the pentacene active layer across shadow mask by thermal evaporation. Their thicknesses were 80 nm (pentacene), and 80 nm (S–D electrodes Au), respectively. All the thin films were grown at low temperature (< 100°C) and low deposition rates (≤ 0.6 Å). Finally, all samples were thermally treated at 80 °C for 120 minutes in the vacuum oven at 1.0×10^{-1} Pa. The output and transfer curve measurements of TC-OTFTs were performed with a KEITHLEY 2410, 6430 and 4200 Source Meter parameter analyser in the dark at room temperature.

In this work we fabricated two-group devices, device 1 and device 2, and the structures are shown in Fig.1. Figures 1(a) and 1(b) are schematic diagrams of the cross-section structures of device 1 and device 2 respectively. Figures 1(c) and (1d) are the chemical structure of the pentacene molecule and a microscope photographic plan view of actual devices, respectively. The inset pattern in Fig.1(d) shows a microscope photographic plan view of the channel for TC-OTFTs devices.

As shown in Figs.1(b), device 2 was optimized on the basis of device 1. An ultra-thin BCP was inserted into the middle of the pentacene active layer. The ultra-thin BCP-HBI was deposited with a rate of 0.03 nm/s by means of thermal evaporation in high vacuum 2×10^{-5} Pa. From the energy level, it can be seen that the function of BCP-HBI is to block holes and form two active layers of 80 nm thickness in a pentacene layer.[13,14]

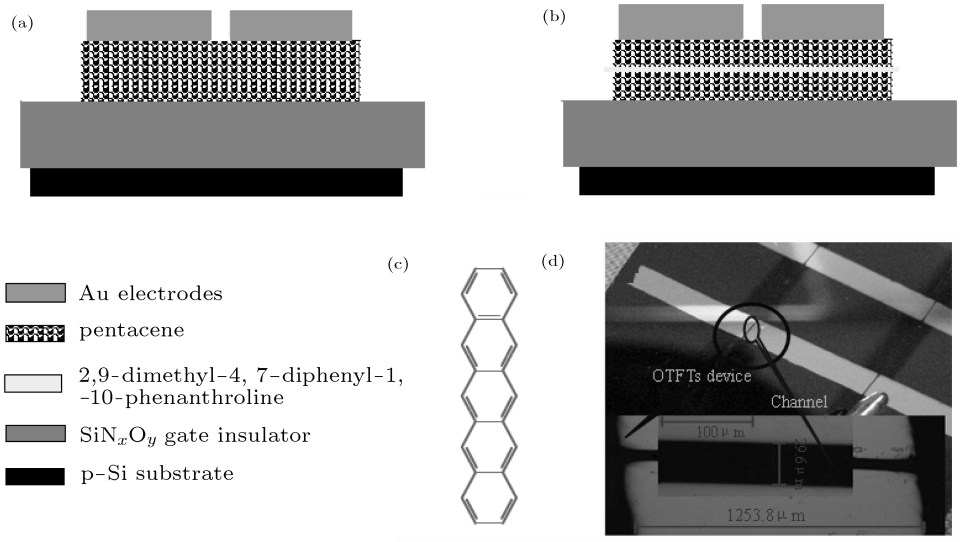


Fig.1. Figures 1(a) and 1(b) are schematic diagrams of device 1 and device 2 cross-section structures, respectively. Figure 1(c) is the chemical structure of the pentacene molecule and Fig.1(d) is a microscope photographic plan view of actual OTFT devices.

Figure 2 shows the output characteristics of OTFT device 1 and device 2 at different gate voltages (V_{GS}), and the two devices show typical P-channel characteristics and good output characteristics. The clear saturation current behaved quadratically as a function of the gate bias and was obtained as shown in Fig.2. The output characteristics of the OTFT device were improved by the insertion of an ultra-thin BCP-HBI into the middle of the pentacene active layer. The output current was increased from 62.24 μA of device 1 to 79.7 μA of device 2 at $V_{GS} = -30$ V.

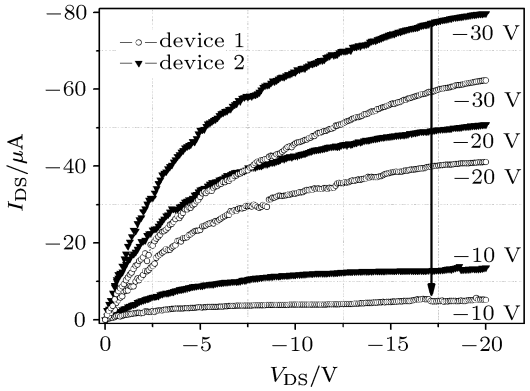


Fig.2. Output characteristics of OTFT device 1 and device 2 at different V_{GS} (–30 V, –20 V, –10 V). The ratio of channel width to channel length W/L was 42.

Figure 3 shows the corresponding transfer characteristics and the curve of the square root of the drain current vs gate voltage for OTFT devices with ultra-thin BCP-HBI at $V_{DS} = -20$ V. The channel length and width are 30 μm and 1254 μm, respectively. From Fig.3, we obtained that the current on/off ratio was increased from 2.8×10^4 of device 1 to 5.52×10^5 of device 2 after the insertion of ultra-thin BCP interlayer, and the threshold voltage (V_{TH}) was decreased from –5.23 V to –4.6 V. In the saturation region $V_{DS} > (V_{GS} - V_{TH})$, the mobility was extracted from

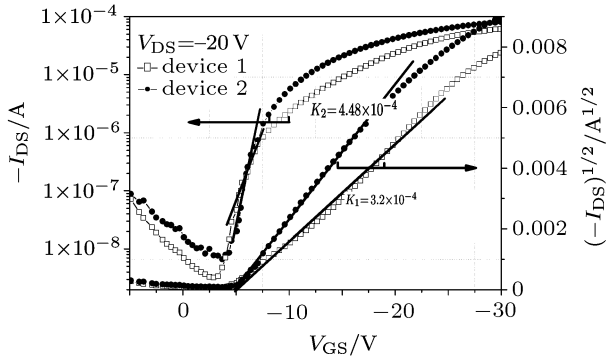


Fig.3. Transfer curve and plot of $\sqrt{I_{DS}}$ vs V_{GS} of OTFT device 1 and device 2 at $V_{DS} = -20$ V, respectively.

the transfer characteristics plotted as $\sqrt{I_{DS}}$ vs V_{GS}. The mobility is calculated using Eq.(1) by solving for μ_{EF}. In the saturation region, $V_{DS} > (V_{GS} - V_{TH})$, I_D is given by

$$I_{DS} = \frac{WC_i\mu_{EF}}{2L}(V_{GS} - V_{TH})^2. \quad (1)$$

The field-effect mobility in the saturation region was extracted from the transconductance of the device. If W, L and C_i are known, the field-effect mobility μ_{EF} was calculated at the saturation regions using the following equation:[15]

$$\mu_{EF} = \frac{2L}{WC_i}\left(\frac{\partial\sqrt{I_{DS}}}{\partial V_{GS}}\right)^2, \quad (2)$$

where W is the transistor channel width, L is the transistor channel length, μ_{EF} is the field-effect mobility, V_{TH} is the threshold voltage, and C_i is the capacitance per unit area of the insulator. The ratio of W/L of the OTFT channel was 1254 μm/30 μm (C_i of a SiO_xN_y insulator with 300 nm thickness is 16.48 nF/cm^2).

The threshold voltage V_{TH} was determined from the intercept of the fitting line with the horizontal axis used to extract the mobility in the saturation region.[16,17] From Eq.(2), a significant improvement of the field-effect mobility μ_{EF} was increased from 0.29 cm^2/(V·s) of device 1 to 0.58 cm^2/(V·s) of device 2 through inserting ultra-thin BCP-HBI. From the results we could obtain that ultra-thin BCP-HBI can efficiently influence the field-effect behaviours of an OTFT device, and the reasons were analysed according to Fig.4.

Figure 4(c) shows that the 5 nm ultra-thin BCP-HBI has a significant block for the hole, because of the higher hole potential barrier of 1.3 eV at the interface between BCP-HBI and pentacene. Consequently, the carriers were divided into two parts and accumulated at the two interfaces of the pentacene/BCP-HBI and pentacene/Si_xO_y insulator, respectively. Finally, double-conductible channels are formed in the device 2, as shown in Fig.4(b). After the BCP was inserted, the carriers were distributed in double-conductible channels, and Coulomb interaction forces impacting and scattering each other between carriers were decreased in comparison with the case without a BCP layer. So the amount of efficient carriers provided for conduction was enhanced, thus increasing the output current of the OTFT device.[4–8]

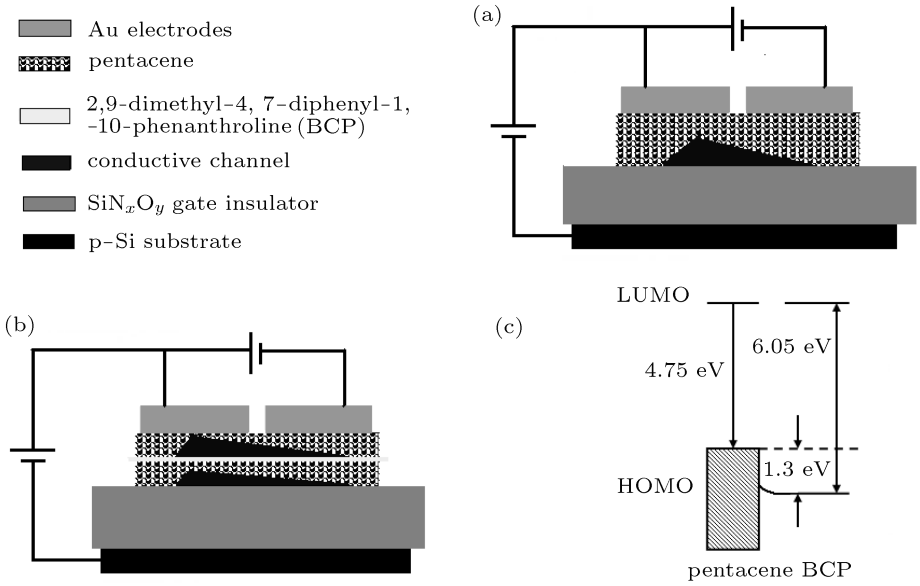


Fig.4. Schematic drawings of the OTFT device. Figure (a) shows single-conductible channels without ultra-thin BCP-HBI for device 1. Figure (b) shows double-conductible channels with ultra-thin BCP-HBI for device 1 and device 2. Figure (c) shows schematic energy level diagrams of the interfaces between pentacene and BCP.

The amount of carriers of the provided conduction was increased. Because they distributed in the double-conductible channel, the Coulomb interaction forces, impacted and scattered due to the accumulation aroused between carriers, were greatly decreased and more carriers disengaged from the group system into the conductible channel; the concentration of carriers was greatly decreased in every conductible channel, and thereby the transport rate of carriers was increased, and the mobility of carriers was enhanced. Finally, we significantly improved the characteristics of OTFT device.

It is known that the thickness of the depletion and accumulation layers for carriers in OTFTs is at the first few molecular layers which are close to the interface between pentacene and the gate insulator. So an ultra-thin BCP-HBI layer is important for OTFT performance.

The significant improvement in the measured mobility and threshold voltage can be attributed to a decreased charge trap density at the pentacene interface.[18,19] We estimated the areal density of interfacial traps in the OTFTs devices using a procedure. Firstly we assume that the difference in threshold voltage of the OTFT device to that of various buffers is due to trapped charge on one side of a capacitor, of a capacitance/area equal to $C_{\rm i}$, method (1) $N_{\rm trap} \sim C_{\rm i} \times \Delta V_{\rm TH}/q$.[20,21] Using method 1, we calculate the interfacial trap density in the octadecyltrichlorosilane (OTS)-treated OTFTs, and obtain a result of 2.5×10^{11}. OTFTs with ultra-thin BCP-HBI result in a corresponding estimated interfacial trap density of 9.68×10^{10}, indicating that the trap states have been limited by ultra-thin BCP-HBI.

4. Conclusions

In this work, a BCP hole-blocking layer has been applied in OTFT to improve its properties by means of the double-conductible channels of pentacene/BCP-HBI and pentacene /Si_xO_y interfaces. The main reasons for this are that a large amount of carriers within the pentacene active layer were distributed at the two interfaces of the pentacene/BCP-HBI and pentacene/Si_xO_y insulator, respectively. The concentration of carriers and Coulomb interaction forces, impacted and scattered between carriers, were greatly decreased when $V_{\rm DS}$ was -20 V, the threshold voltage, current on/off ratio, field-effect mobility of TC-OTFTs with an ultra-thin BCP hole-blocking interlayer were –4.6 V, 5.52×10^5 and 0.58 $cm^2/(V{\cdot}s)$, respectively.

References

[1] Yamaguchi K, Takamiya S, Minami M, Doge Y, Nishide Y, Osuga H, Uno K and Tanaka I 2008 *Appl. Phys. Lett.* **93** 043302

[2] Torsi L, Farinola G, Marinelli F and Tanese M C 2008 *Nature Mater.* **2169** 412

[3] Yang C, Yoon J, Kim S H, Hong K, Chung D S and Heo K 2008 *Appl. Phys. Lett.* **92** 243305

[4] Yuan G C, Xu Z, Zhao S L and Zhang F J 2008 *Acta. Phys. Sin.* **57** 5911 (in Chinese)

[5] Alves H, Molinari A S, Xie H and Morpurgo A F 2008 *Nature Mater.* **2205** 574

[6] Calhoun M F, Hsieh C and Podzorov V 2007 *Phys. Rev. Lett.* **98** 096402

[7] Matsui H, Hasegawa T and Tokura Y 2008 *Phys. Rev. Lett.* **100** 126601

[8] Yuan G C, Xu Z, Zhao S L and Zhang F J 2008 *Chin. Phys.* B **17** 3822

[9] Jo'zsa C, Popinciuc M, Tombros N, Jonkman H T and Wees B J V 2008 *Phys. Rev. Lett.* **100** 236603

[10] Klauk H, Halik M, Zscieschang U, Schmid G and Radlik W 2002 *J. Appl. Phys.* **92** 5259

[11] Lee S, Koo B, Shin J, Lee E, Park H and Kim H 2006 *Appl. Phys. Lett.* **88** 162109

[12] Chou W Y, Kuo C W, Cheng H L, Chen Y R, Tung F C and Yang F Y 2006 *Appl. Phys. Lett.* **89** 112126

[13] Divayana Y, Chen B J and Sun X W 2006 *Appl. Phys. Lett.* **88** 083508

[14] Yu G, Xu X, Liu Y, Jiang Z, Yin S, Shuai Z and Zhu D 2005 *Appl. Phys. Lett.* **87** 222115

[15] Yuan G C, Xu Z, Zhao S L and Zhang F J 2008 *Chin. Phys.* B **17** 1887

[16] Zhang J, Wang J, Wang H and Yana D 2004 *Appl. Phys. Lett.* **84** 142

[17] Gundlach D J, Zhou L, Nichols J A, Jackson T N, Necliudovc P V and Shur M S 2006 *J. Appl. Lett.* **100** 024509

[18] Sayeef S and Supriyo D 2008 *Nano Letters* **8** 405

[19] Manabu K, Manabu N, Toshihiro S and Koichiro S 2005 *Phys. Rev.* B **71** 035332

[20] Rolland A, Richard J, Kleider J P and Mencaraglia D 1993 *J. Electrochem. Soc.* **140** 3679

[21] Wang X, Ouyang Y, Li X, Wang H, Guo J and Dai H 2008 *Phys. Rev. Lett.* **100** 206803